

Vertical spatial scales of ice supersaturation and probability of ice supersaturated layers in low resolution profiles of relative humidity

N.C. Dickson¹, K. Gierens^{2*}, H.L. Rogers¹, R.L. Jones¹

1) *Centre for Atmospheric Science, University of Cambridge, Cambridge, UK*

2) *DLR Oberpfaffenhofen, Institut für Physik der Atmosphäre, Germany*

Keywords: Ice supersaturated regions, Radiosondes

ABSTRACT: We present an analysis of the vertical extension of ice supersaturated regions based on high resolution, corrected humidity data from British radiosonde launch stations (2002-2006). Additionally, we provide a probabilistic description of the occurrence of ice supersaturated layers in low resolution profiles of relative humidity. The results bear an importance for operational strategies of contrail avoidance.

1 INTRODUCTION

To avoid formation of persistent contrails means to avoid flights through ice supersaturated regions (ISSRs). Based on an analysis of the vertical extension of ISSRs obtained from 14 months of radiosonde data from Lindenberg, Germany, Mannstein et al. (2005) proposed that a substantial fraction of flights in ISSRs can be avoided by changing flight levels by 1-2 levels, because the supersaturated layers over Lindenberg turned out to be shallow on average (about 650 m). However, radiosonde data from Spitzbergen (Treffeisen et al., 2007) and southern England (Rädel and Shine, 2007) seem to indicate larger vertical extensions of ISSRs which would render the Mannstein et al. avoidance strategy more difficult to implement or less successful. We present new statistical evidence for ISSR vertical extent, utilising in-situ observations from UK Met Office high resolution radiosonde stations. We show layer depth statistics and demonstrate that over this extended data set most ISSR layers are fairly shallow. Hence the avoidance strategy of Mannstein et al. can well be confirmed; however, for weather prediction models with their usually low resolution layers in the tropopause region it will be more difficult to correctly predict ISSRs unless their vertical resolution is improved. In order to estimate the true occurrence frequency of ISSRs in low resolution data, we additionally derive from the radiosonde data set a probabilistic description of the occurrence of ice supersaturated layers in low resolution profiles of relative humidity.

2 PROCESSING OF RADIOSONDE DATA

2.1 Selection of launch stations

From the UK Met Office global radiosonde data-set we selected a sub-set of nine radiosonde stations, sited predominantly around the UK but with three non-UK stations (Gibraltar, St. Helena and the Falkland Islands) that have recorded vertical profiles at a high vertical resolution, i.e. every two seconds. Profiles for a five year period, from 1st January 2002 to 31st December 2006, from nine UK Met Office radiosonde launch stations as shown in Table 1, were used to study the vertical extent of ISS layers. For the nine stations used, launches were typically twice daily at local times of 1200h and 2400h. The only exception to this was St. Helena, which recorded approximately one launch per day, with approximately 20-25 launches per month.

* *Corresponding author:* Klaus Gierens, DLR-Institut für Physik der Atmosphäre, Oberpfaffenhofen, D-82234 Wessling, Germany. Email: Klaus.Gierens@dlr.de

Table 1: A summary of UK Met Office high resolution radiosonde observations (1st January 2002 to 31st December 2006) used in this study. Observations were generally performed using the Vaisala RS80 up to mid-2005 with the RS92 instrument used thereafter [UK Met Office].

Station	Location	Launches (2002-06)	Radiosonde type
Albemarle	1.88°W, 55.02°N	3546	RS80/RS92
Camborne	5.329°W, 50.218°N	3981	RS80/RS92
Castor Bay	6.503°W, 54.503°N	3234	RS80/RS92
Herstmonceux	0.319°E, 50.89°N	3771	RS80/RS92
Lerwick	1.183 °W, 60.139°N	3957	RS80/RS92
Watnall	1.25 °W, 53.005°N	3804	RS80/RS92
Gibraltar	5.35°W, 36.15°N	3429	RS80
St Helena	5.667°W, 15.933°S	1189	RS80
Falkland Islands	58.45°W , 51.817°S	3551	RS80

2.2 Correction

The Vaisala RS80-H radiosonde was in service with UK Met Office launch stations until approximately mid-2005, when the RS92 type radiosonde entered service. The exact changeover date was launch station dependent, but from the beginning of 2006 all observations used here were made with the RS92 radiosonde. Both RS80 and RS92 are subject to different systematic errors and as such these instruments have different correction algorithms. The RS80-H has specific issues over temperature dependency, chemical contamination, sensor ageing and measurement time lag, leading to a dry bias. To account for the resulting bias in observations, the correction presented by Wang et al., (2002) was used. RS92 observations are also subject to a dry bias, in this case due to the lack of a radiation shield, leading to solar heating of the humidity sensor [Vömel et al., 2006]. There is less information regarding RS92 accuracy and only a few correction methods are available, however, a study by Vömel et al., (2006) was applied here to correct for the observation dry bias. It is worthy of note, that in many profiles, ISS events would not be observed if it were not for application of the correction algorithms [see also Rädcl and Shine, 2007]. Data contaminated by sensor icing and data from pressure layers containing the tropopause have been discarded from the study.

3 RESULTS

3.1 Occurrence of ice supersaturation

Figure 1a describes the seasonal changes with relation to launch station and the inter-annual variation, respectively, from stations in the British Isles. These data show that ISS, of any layer thickness, is likely to occur with a probability of between 13% and 25% in the winter and 9% and 17% in the summer. These statistics are similar to those presented in Rädcl and Shine (2007) which presents ISS events occurring at a frequency of 15-25% and 9-12% in the winter and summer respectively. Occurrence of ISS and seasonal trends in the troposphere, presented in Rädcl and Shine (2007) and Vaughan et al (2006), support the findings here.

The same analysis is performed on the data from stations outside of the British Isles. 1b shows the ISS occurrence statistics from the St Helena, Gibraltar and Falkland Islands stations and is compared to the monthly mean from the six British Isles based stations. St Helena demonstrates a low occurrence of ISS, and this can not simply be explained by the paucity of data from this station. The Gibraltar and Falkland Island stations show variation in the monthly mean in line with expectations.

Gibraltar shows in general a smaller probability of ISS occurrence compared with the British Isles stations, but with a summer low of two percent and a winter high of 13% the seasonality trends are similar. The Falkland Islands, with its southerly mid-latitude location shows similar lows and highs in the same season, albeit south hemisphere season, as the British Isles data.

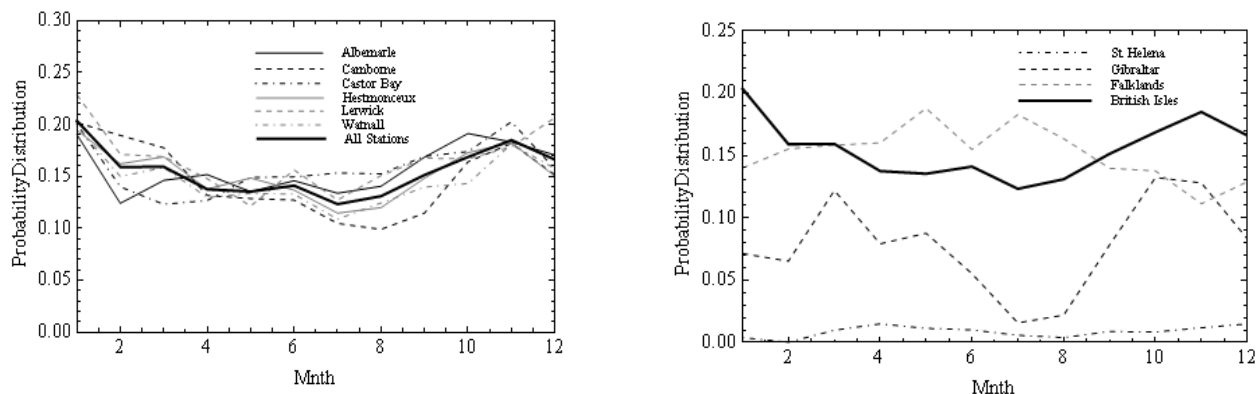


Figure 1. (a) Frequency of occurrence of ice supersaturated layers in radiosonde profiles from 6 launch station on the British Isles; (b) same as (a) but for Gibraltar, St Helena and the Falkland Islands.

3.2 Vertical extension of ice supersaturated layers

To investigate the vertical extensions of ISSRs and their statistics, each radiosonde profile is interrogated for ISS. Once an ISS event is identified then the depth is recorded. The British Isles dataset is used (2002–2006) to generate a radiosonde station centric subset of ISS events. These subsets are divided into bins of 100 metre layer depths and initially this gives a frequency distribution as described by 2. The difference between stations is remarkably small and there is evidence of an exponential-type distribution. The majority of layers are shallower than 1500m, accounting for 81 to 87 percent of data and 27 to 34 percent of layers are less than 100 metres deep. The remaining layers occur in sizes up to 4500 metres with on average 11 percent are in the size range 1500 to 3000 metres and with 5% greater than 3000 metres. The distributions are similar for the three considered launch stations outside the UK, and the annual and seasonal variations are weak except for the shallowest layers.

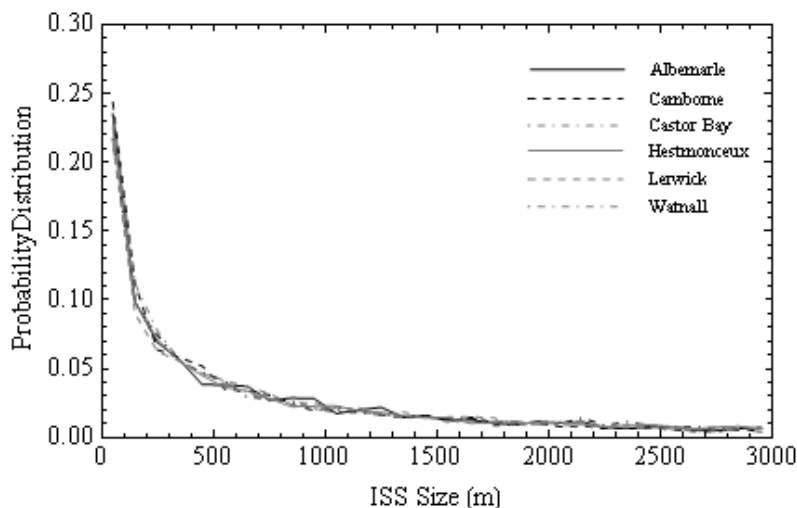


Figure 2. Probability distribution function of vertical layer depths of ice supersaturated layers detected in radiosonde humidity profiles at 6 launch station in the UK.

3.3 Probabilistic description of the occurrence of shallow ice supersaturated layers embedded in low-vertical resolution humidity profiles

The analysis was based on 30,462 radiosonde profiles separated into 50 and 100 hPa layers which gave totals of 152,310 50 hPa and 60,924 100 hPa pressure layers. For each pressure layer we determined the fraction of single humidity measurements that showed ice supersaturation in that layer together with the average relative humidity over that layer. The relation between these quantities is shown in Figure 3.

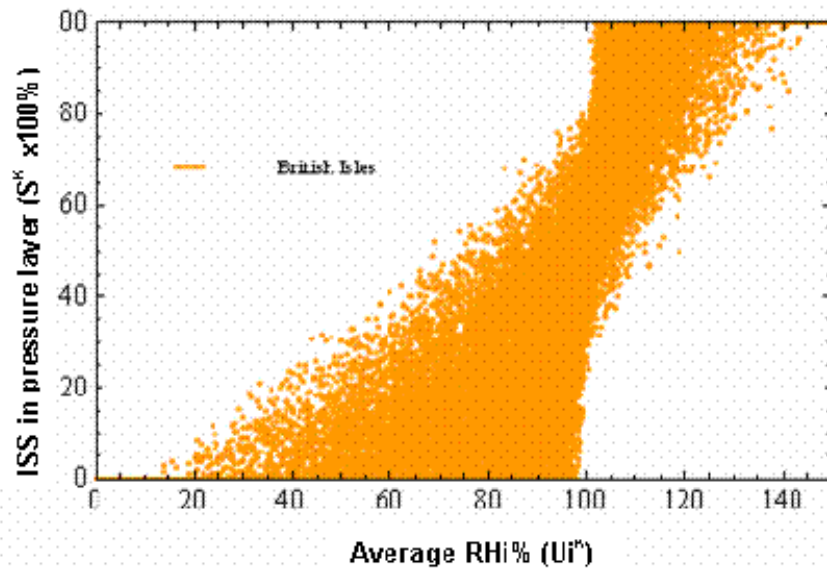


Figure 3. The fraction of humidity measurements indicating ice supersaturation vs. the corresponding average relative humidity wrt ice for 50 hPa pressure layers over the British Isles.

These data have been grouped together in 5% RHi bins, and the mean of the fractional ISS occurrence has been computed for each bin. This resulted in the following s-shaped relationship:

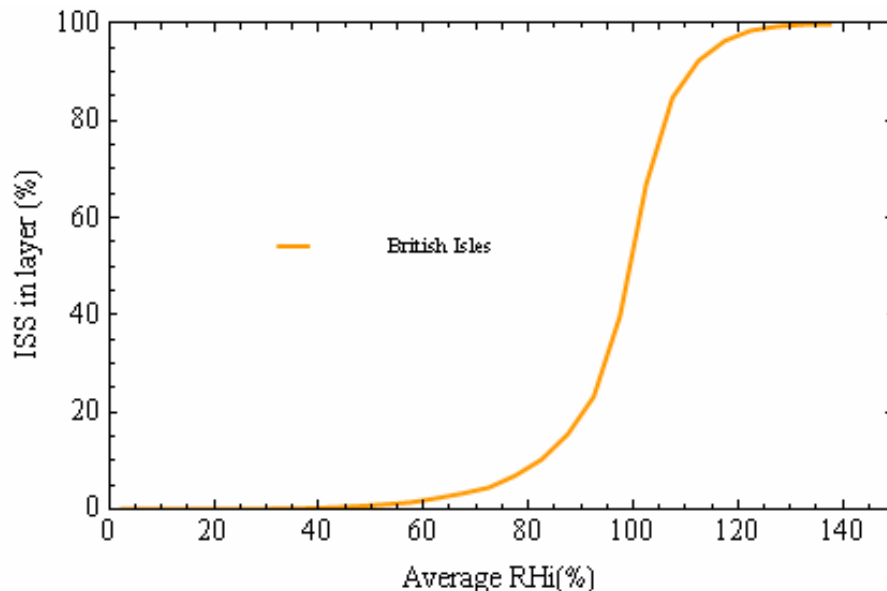


Figure 4. The average fraction of ice supersaturation in thick layers vs. the average RHi in that layer displays an s-shaped relation.

The maximum standard deviation from the s-curve is 0.18, determined from the whole British Isles data set. In comparison to this, variations due to geographical location, annual and seasonal variation, and vertical location of the considered pressure layer, are all smaller, such that this s-curve can be considered as representative for all cases. We have additionally developed a simple mathematical description of the s-curve, based on the observed data. This will be presented elsewhere.

4 CONCLUSIONS

After analysing 5 years of high-vertical resolution radiosonde humidity profiles obtained from 9 launch stations on the British Isles and three from elsewhere (Gibraltar, St Helena, and Falkland Islands) we arrived at the following results:

- Ice supersaturated layers occur on average in 15–20% of all radiosonde profiles over the British Isles and the Falkland Islands, i.e. mid-latitude stations. The ISS frequency is very low at the tropical site of St Helena, and intermediate at Gibraltar.

- The vertical extension of ice supersaturated layers obeys a roughly exponential probability distribution; that is, most layers are shallow, such that aircraft can often avoid flying in ice supersaturated air by switching their flight level by one standard step up or down.
- Humidity profiles in low vertical resolution, e.g. from radiosonde archives (standard pressure levels) or from satellite data can be corrected to determine a probable ISS frequency using the s-shaped relationship derived from the data. The mathematical model that we have developed will simplify such an exercise.

These results bear some implications not only for strategies of operational contrail avoidance, as indicated, but also for (aviation) weather forecast which must be able to reliably predict ice supersaturated layers. The predominant shallowness of these layers makes it necessary either to improve the vertical resolution of weather models in the upper troposphere region (which will occur as soon as computer power allows it) or to introduce means and measures that describe the vertical sub-grid scale variability. The latter is in particular worth of consideration in climate models with their generally lower vertical resolution. The application of the s-shaped relationship may be a way forward into this direction.

5 ACKNOWLEDGEMENT

This research was funded by the UK research council NERC at the University of Cambridge, in collaboration with QinetiQ, and was supported by the DLR project CATS. It contributes further to the German UFO project and to the European Network of Excellence ECATS.

REFERENCES

- Mannstein, H., P. Spichtinger, and K. Gierens, 2005: A note on how to avoid contrails. *Transportation Res. Part D* 10, 421-426.
- Rädcl, G., and K.P. Shine, 2007: Evaluation of the use of radiosonde humidity data to predict the occurrence of persistent contrails. *Quart. J. Roy. Meteorol. Soc.*, 133, 1413-1423.
- Treffeisen, R., R. Krejci, J. Ström, A.C. Engvall, A. Herber, and L. Thomason, 2007: Humidity observations in the Arctic troposphere over Ny-Alesund, Svalbard based on 15 years of radiosonde data. *Atmos. Chem. Phys.*, 7, 2721-2732.
- UK Meteorological Office, 2006: UK High Resolution Radiosonde Data, [Internet]. British Atmospheric Data Service (BADc). Available from <http://badc.nerc.ac.uk/data/rad-highres/>
- Vömel, H., H. Selkirk, L. Miloshevich, J. Valverde-Canossa, J. Valdés, E. Kyrö, W. Kivi, W. Stolz, G. Peng, J.A. Diaz, 2007: Radiation dry bias of the Vaisala RS92 humidity sensor. *J. Atmos. Ocean. Techn.*, 24, 953-963.
- Wang, J.H., H.L. Cole, D.J. Carlson, E.R. Miller, K. Beierle, A. Paukkunen, T.K. Laine, 2002: Corrections of humidity measurement errors from the Vaisala RS80 radiosonde - Application to TOGA COARE data. *J. Atmos. Ocean. Techn.*, 19, 981-1002.

Impact on air quality of a 90 km/h speed limit during PM10 episodes

P. Viaene^{*}, W. Lefebvre, K. Van de Vel, S. Janssen, G. Cosemans, K. De Ridder, I. De Vlieger, C. Mensink, L. Schrooten, J. Vankerkom
VITO, Mol, Belgium

F. Fierens
Belgian Interregional Environment Agency, Brussels, Belgium

T. Van Mierlo
Flemish Government Department of Environment, Nature and Energy, Section Air and Climate, Brussels, Belgium

F. Blommaert
Flemish Environmental Agency, Antwerp, Belgium

Keywords: road transport, smog, emission reduction

ABSTRACT: During smog episodes Flemish legislation imposes a 90 km/h speed limit on certain stretches of the highway network. In this contribution to TAC-2 we present the results of a study in which we assess the effects of this measure on air quality and compare the effect to other more stringent measures such as banning heavy duty vehicles or cars older than EURO-3 from the highways.

1 INTRODUCTION

To protect the health of its citizens the European Community has defined air quality guidelines to limit particulate matter (PM₁₀) concentrations such as the “cleaner air for Europe” directive (2008/50/EG) which states that the daily average PM₁₀ concentration may not exceed 50 µg/m³ for more than 35 days a year. According to Article 24 of this directive, EU member states have to devise action plans stating which type of actions are taken in case threshold values are likely to be exceeded, in order to diminish both the risk and the duration of such exceedances. Within this context the Flemish government decided to adopt a speed limit of 90 km/h instead of 120 km/h on certain high way sections during PM₁₀ smog episodes.

2 METHODOLOGY

To assess the effect of the speed limit measure and compare this effect to that of more severe measures the air quality during 2 smog episodes was modelled for a reference situation where no speed limit is imposed and a number of scenario's using a suite of models (Figure 1) that can calculate the effect of different emission scenario's on air quality in enough detail to discern the short range effects that are to be expected.

Besides the reference run using the normal emissions, the study considered the following scenario's:

- the speed limit is reduced to 90 km/h in line with Flemish legislation to a selection of the highway network;
- the speed limit of 90 km/h is applied to all the highways in Flanders and Brussels;
- scenario 1 and all heavy duty vehicles of euro-classes 0, 1 and 2 are banned and not replaced by newer heavy duty vehicles;
- scenario 1 and all heavy duty vehicles are taken off the road;

^{*} *Corresponding author:* Peter Viaene, VITO, Boeretang 200, B-2400 Mol, Belgium. Email: peter.viaene@vito.be

- scenario 1 and all cars, of euro-classes 0, 1 and 2 are taken off the road and not replaced by newer vehicles.

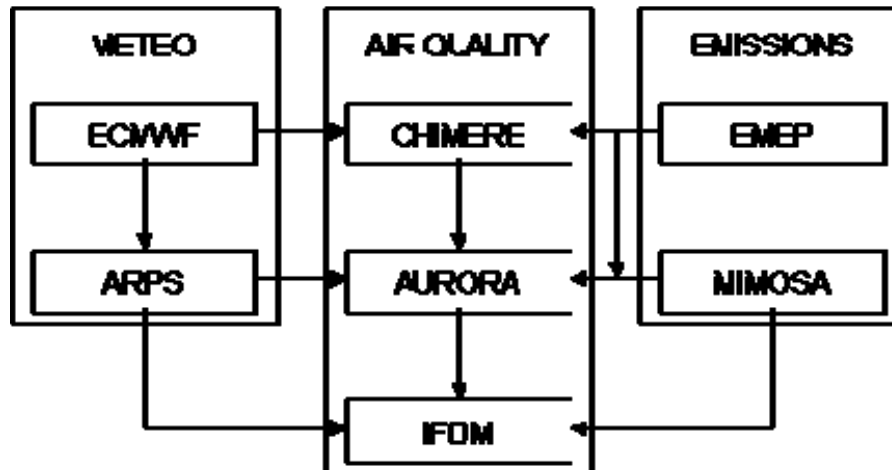


Figure 1. The coupled modelling system used for this study.

3 EMISSIONS

For the road traffic emissions, MIMOSA4 the most recent version of the MIMOSA model (Mensink et al., 2000, Vankerkm et al., 2005) was used. This model generates hourly traffic emissions for different types of pollutants, such as PM₁₀ and PM_{2.5} for Flanders. Based on the modelled number of different types of vehicles for each road, MIMOSA calculates the corresponding emissions by splitting up the total number of vehicles into different categories, depending on e.g. weight, EURO class, ... This distribution is based on statistical data on the vehicle fleet in Flanders. In order to calculate these emissions, the COPERT-IV methodology has been used. Emissions due to cold start and loss by evaporation are also modelled and for particulate matter the model takes into account non-tailpipe emissions due to brake-, tire- and road wear.

The MIMOSA model sets the traffic speed based on the type of road (rural, urban, highway,...). For the purpose of this study, the model was adapted so that different speed limits can be imposed for different parts of the road network. The speed limits can also be specified for individual EURO classes and vehicle types in order to allow for maximum flexibility in the scenario definition.

In the study we also looked at elementary carbon (EC). As EC is not modelled by MIMOSA the EC emissions were estimated from the PM_{2.5} emissions by multiplying these by 0.7. This high fraction is reasonable in view of the fleet composition in Flanders where the vast majority of cars has a diesel engine.

For the non-traffic emissions, the EPER-database is used, except for Flanders. For this last region, the emissions are those from the Emissie-Inventaris Lucht (EIL), the so-called ‘Kernset’. More information on the used emissions can be found in Maes et al. (2009).

The reduction in the average emission for each of the scenario’s can be found in Table 1 below.

Table 1. The mean traffic emissions for NO_x, PM₁₀ and PM_{2.5} for the different scenario's relative to the emission for the reference run in % of the reference values.

	NO _x	PM ₁₀	PM _{2.5}
Scenario 1	95.91	94.04	93.15
Scenario 2	91.28	87.32	85.43
Scenario 3	81.64	86.42	84.63
Scenario 4	52.07	76.17	73.52
Scenario 5	81.42	70.54	69.73

4 AIR QUALITY MODELLING

For the air quality modelling both the AURORA and the IFDM models were used. The AURORA air quality model (Mensink et al., 2001) is a prognostic 3-dimensional Eulerian chemistry-transport model, designed to simulate urban- to regional-scale concentration fields. The IFDM model (Cosemans et al., 1992) on the other hand is a bi-Gaussian plume model used to describe the local dispersion of traffic emissions. The modelling approach consists of a number of one way nested runs starting with the boundary condition and initial conditions from a regional model run for a domain covering Europe at a resolution of 25 km over intermediate resolutions of 15 and 9 km to arrive at modelling results for a resolution of 3 km for the Flemish region. The 3 km AURORA concentrations are then after correction for the road emissions taken as background concentrations for runs with the IFDM model. To obtain detailed results along the highways the IFDM run calculates results for the points of a 1 km resolution regular grid combined with those of an irregular grid along the roads with a resolution varying from 50 to 800 m. The meteorological input required for the air quality modelling at the different resolutions was calculated with the ARPS model (Xue et al., 2000).

As can be expected the improvement of the average air quality in Flanders due to limiting the speed on selected stretches of the highways to 90 km/h is rather small. For this scenario the concentrations of NO₂ and PM are reduced by less than one percent (Table 2). The effect on the concentrations is more pronounced along the highways (Figure 2) where the concentration decreases up to 8% for NO₂ and 3% for PM. In this study we also looked at the changes in the elementary carbon concentration. Here we found a reduction of up to 30% in the immediate vicinity of highways and of 10% up to 1.2 km away from the highway.

Table 2. The percent change in average concentration for Flanders in NO₂, PM₁₀ and PM_{2.5} for the different scenario's relative to the reference run.

	NO ₂	PM ₁₀	PM _{2.5}
Scenario 1	-0.87	-0.12	-0.22
Scenario 2	-1.87	-0.26	-0.50
Scenario 3	-7.60	-0.45	-0.80
Scenario 4	-10.91	-0.54	-0.95

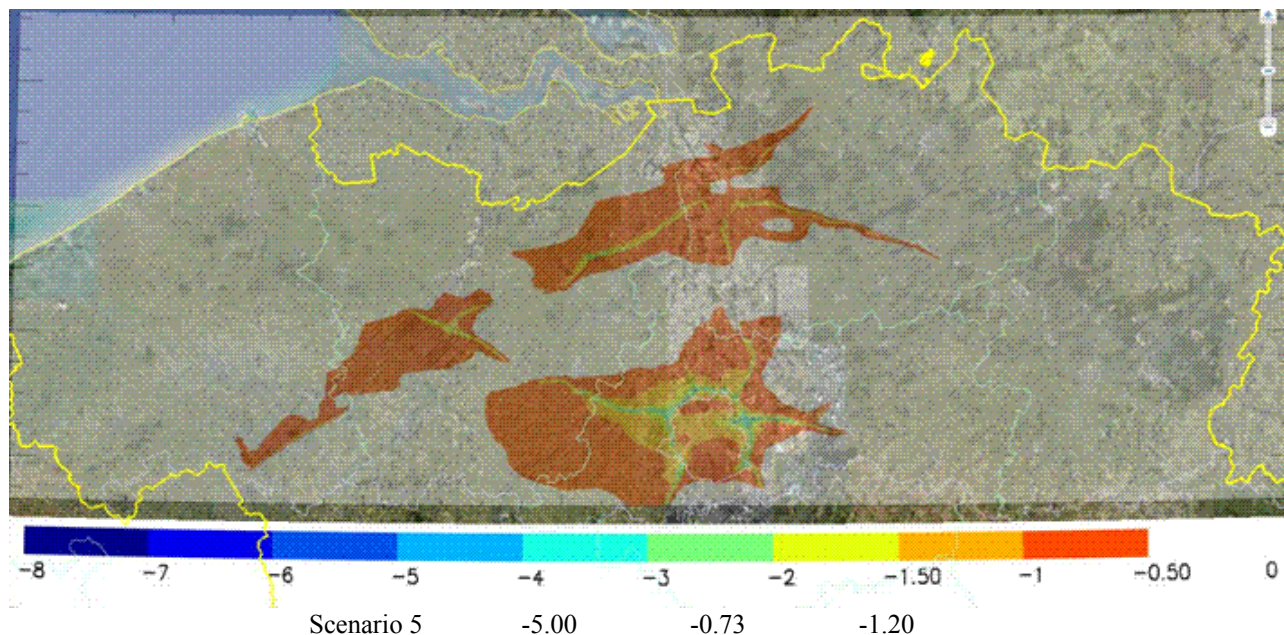


Figure 2. Percent change of the average modelled PM_{2.5} concentration for scenario 1 compared to the reference situation for the whole smog episode of December 2007.

By combining the modelled concentration changes with a population density map, one can also assess the changes in population exposure as shown in Figure 3. It can then be seen that scenario 1 results in a 0.5% decrease in PM_{2.5} concentration for 50 % of the population. For 5% of the population the PM_{2.5} concentration decreases by 1.3%.

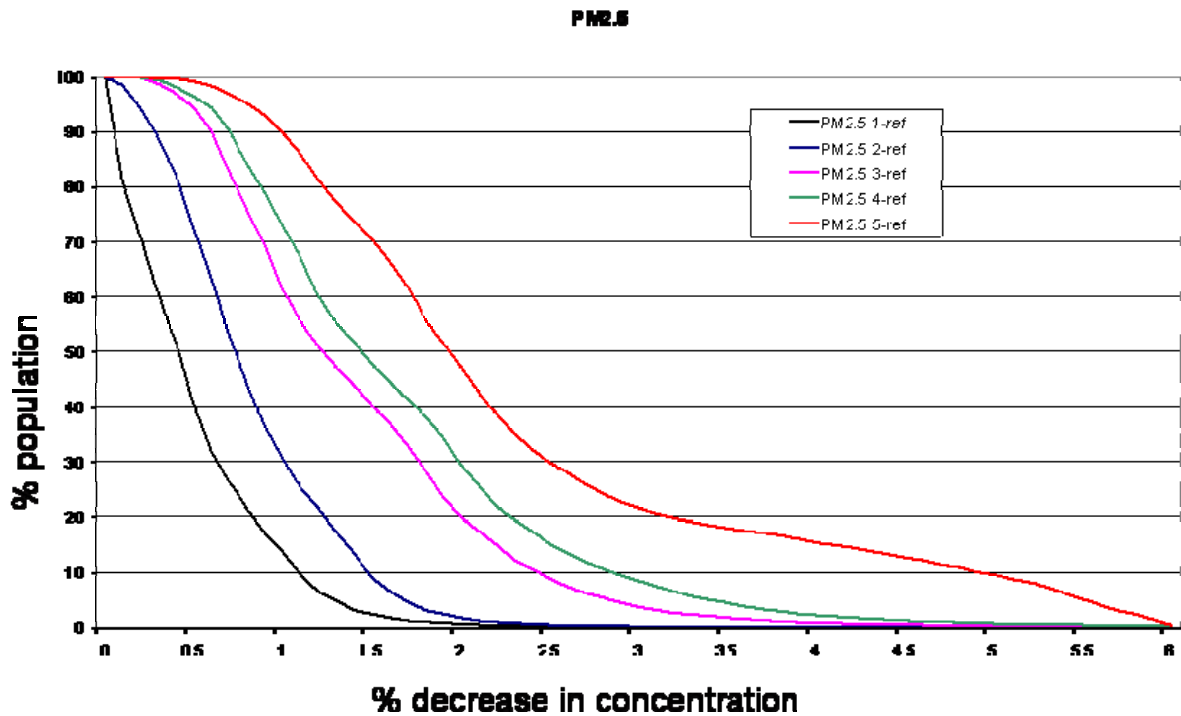


Figure 3. Percentage of the population for which a certain decrease in concentration of PM_{2.5} is valid for the different scenario's.

5 CONCLUSIONS

According to the results of this study enforcing a speed limit of 90 km/h on some of the high ways in Flanders during smog episodes has a limited effect on PM and NO₂ concentration levels for the region as a whole. The effect is however more significant if one accounts for the fact that the population density can be high along highways and if we focus on elementary carbon which is believed to be one of the more detrimental components of PM. In general this study demonstrates that modelling tools can help the administration to evaluate and compare different policies for improving air quality.

REFERENCES

- Cosemans, J., Kretzschmar J., Maes G., 1992: The Belgian Immission Frequency Distribution Model IFDM Proceedings of the DCAR workshop on objectives for the next generation of practical short range atmospheric dispersion models. May 6-8, 1992, Risoe, Roskilde, Denmark.
- Maes, J., Vliegen, J., Van de Vel, K., Janssen, S., Deutsch, F., De Ridder, K., Mensink, C., 2009: Spatial surrogates for the disaggregation of CORINAIR emission inventories, Atmospheric Environment, Volume 43, Issue 6, February 2009, 1246-1254.
- Mensink, C., De Ridder, K., Lewyckyj, N., Delobbe, L., Janssen, L., Van Haver, P., 2001: Computational aspects of air quality modelling in urban regions using an optimal resolution approach (AURORA). Large-scale scientific computing – lecture notes in computer science, 21791, 299-308.
- Mensink, C., De Vlioger, I. and Nys, J., 2000: An urban transport emission model for the Antwerp area. Atmospheric Environment, 34, 4595-4602.
- Naser, T.M., Kanda, I., Ohara, T., Sahamoto, K., Kobayashi S, Nitta, H. and Nataami, T., 2009: Analysis of traffic-related NO_x and EC concentrations at various distances from major roads in Japan, Atmospheric Environment, 41, 2379-2390, doi:10.1016/j.atmosenv.2009.02.002
- Vankerkom, J., Lefebvre, F., De Vlioger, I., Cornelis, E., Schrooten, L., Peetermans, E., Puttemans, C. and Verlinden, K., 2005: Gecombineerd gebruik van verkeerstellingen en TRIPS/32 modeloutput binnen MIMOSA: implementatie, validatie en afstemming met TEMAT en FOD mobiliteit (MIMOSA 3), Studie uitgevoerd in opdracht van ANIMAL, 2005/IMS/R/168, VITO, Mol, Belgium.
- Xue, M., Droegemeier, K. K. and Wong, V., 2000: The Advanced Regional Prediction System (ARPS) - A multiscale nonhydrostatic atmospheric simulation and prediction tool. Part I: Model dynamics and verification. Meteor. Atmos. Physics., 75, 161-193.